

Actuator Control for a Hybrid Suspension System

Guido Koch*, Enrico Pellegrini, Sebastian Spirk, Nils Pletschen and Boris Lohmann

Institute of Automatic Control, Technische Universität München

Boltzmannstr. 15, D-85748 Garching, Germany

Abstract

This report presents actuator control concepts for a new structure of a mechatronic suspension system entitled *hybrid suspension*, which includes a combination of a semi-active damper and a low bandwidth actuator integrated in series to the primary spring and can potentially achieve a performance similar to a fully active suspension system. An overview on the design and constructive realization of the hybrid suspension based on actuator components from production vehicles is given. Models and control approaches for the two integrated actuators are derived and the integration of the hybrid suspension in a quarter-car test rig is presented.

Keywords: Vehicle suspension; Active and semi-active suspensions; Quarter-car test rig; Tracking control; Hydraulic systems.

1 Introduction

Mechatronic suspension systems are integrated in vehicles in order to enhance ride comfort as well as ride safety. The systems can be distinguished into semi-active systems (e.g. variable dampers), slow active systems with an actuator integrated in series to the primary spring and fully active systems with an actuator in parallel to the primary spring and a bandwidth of more than 20 Hz (see e.g. [13]). Figure 1 depicts the corresponding quarter-car models of the systems, where the actuator configurations are integrated between the sprung (a quarter of the chassis mass) and the unsprung mass (primarily wheel, tire and brake mass of one vehicle corner) of the vehicle [9]. In production vehicles with mechatronic suspension systems, mostly semi-active damping systems are integrated due to their low energy demand, their low weight and high control bandwidths. However, the performance of semi-active dampers is limited due to the passivity restriction of the damper force [1].

The authors have shown in [5] that an adaptively controlled suspension system containing a low bandwidth hydraulic actuator in series to the primary spring as well as a continuously variable damper can provide similar ride comfort enhancements as a fully active suspension system. This is accomplished without violating constraints on the dynamic wheel load and suspension deflection due to the adaptive suspension control concept, that modifies the dynamic behavior of the suspension system in order to maximize ride comfort for the current driving state [4]. Due to the fact that this suspension type contains active and semi-active actuator types the authors refer to the new suspension concept as *hybrid suspension* (Figure 1 right). The proposed actuator combination has the advantages of lower costs, lower energy demands

*Corresponding author's email adress: guido.koch@mytum.de

compared to a high bandwidth active system and the fact that the actuator types are already available in production vehicles. In [6] and [4] a suitable adaptive control approach for the *hybrid suspension* has been presented and the advantages of the hybrid suspension have been experimentally validated on a quarter-car test rig designed by the authors.

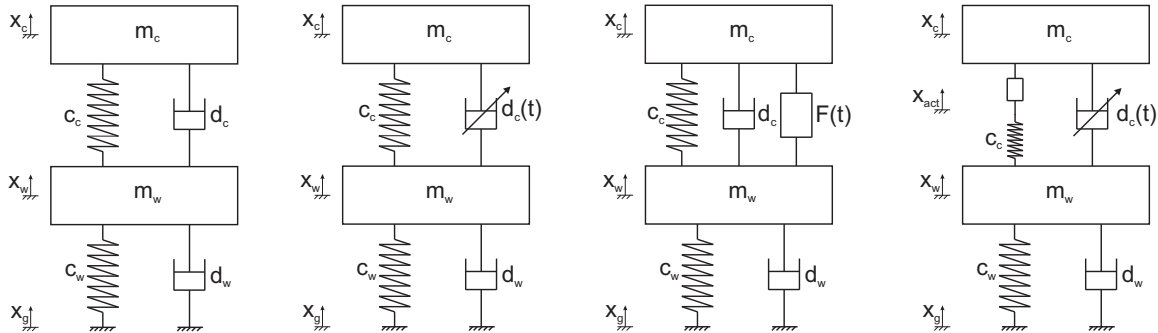


Figure 1: Quarter-vehicle models of a passive, semi-active, fully active and the hybrid suspension system.

This report presents the hybrid suspension system in more detail with an emphasis being given on the description of the actuator modeling and control concepts. Measurement data visualizing the model quality and the actuator performance is presented. Moreover, the quarter-car test rig designed to validate the performance of the hybrid suspension system is presented with a focus on the integration of the suspension strut.

The report is organized as follows: The design of the hybrid suspension strut based on the requirements of the system is described in Section 2. In Section 3 the modeling and a control approach for the actuators are presented and Section 4 describes the quarter-car test rig structure the hybrid suspension strut is integrated in. A conclusion and an outlook on future work is given in Section 5.

2 Design of the hybrid suspension

A requirement for the design of the hybrid suspension has been that only stock hardware from production vehicles should be used to emphasize the realizability of the concept. The hardware components for the considered hybrid suspension design are depicted in Figure 2: A modern hydraulic continuously variable hydraulic damper from the *BMW 7 series* (model year 2009) and a hydraulic suspension actuator integrated in series to the primary spring from the *Active Body Control System (ABC)* of a *Mercedes SL roadster* (model year 2003) (see [11] for more information on the *Mercedes Benz ABC* system).



Figure 2: Continuously variable damper (*BMW 7 series*) and components from the hydraulic *Mercedes Benz - Active Body Control* suspension system.

The hydraulic actuator strut offers a maximum actuator displacement of ± 4 cm and is fixed on the semi-active damper by a connection element. Since the original suspension of the *Mercedes*

SL roadster has a lower transmission ratio (ratio of the relative velocity at the suspension elements and the relative velocity of chassis and wheel mass [8]) than the *BMW 7 series* suspension, the spring of the *Mercedes Benz* is not suitable for the double wishbone suspension configuration of the *BMW*, serving as framework for the hybrid suspension. Therefore, a new spring is integrated, which exhibits the same stiffness characteristic as the original *BMW* spring but preserves the kinematic relations despite the superimposed deflections of the hydraulic actuator. Figure 3 shows the CAD based design and the realization of the hybrid suspension strut.

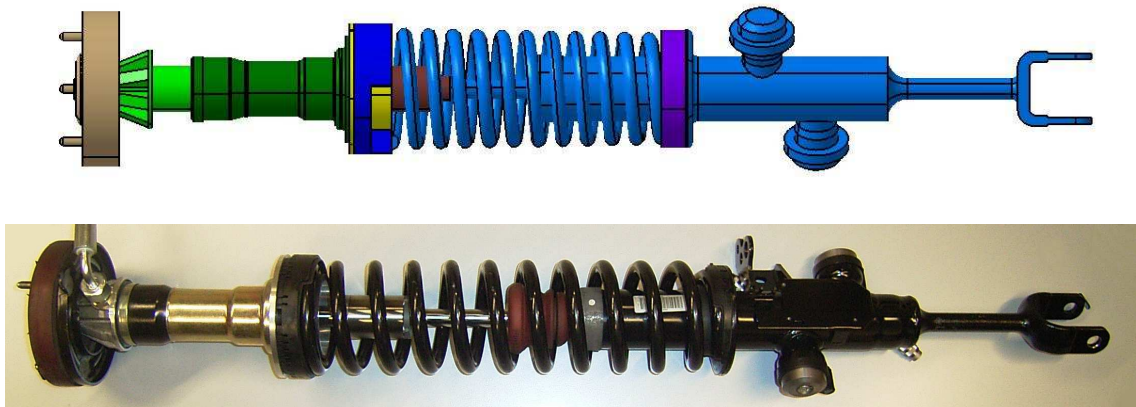


Figure 3: Concept (upper) und realization (lower) of the hybrid suspension.

2.1 Low bandwidth actuator

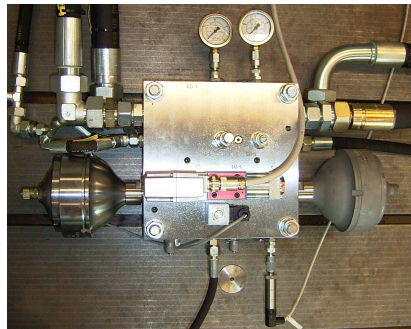


Figure 4: Valve block with pressure accumulators and pressure sensor (upper).

For the hydraulic power supply of the actuator, the same pump, which supplies the hydraulic cylinder emulating the road excitation at the test rig, is used. To control the hydraulic actuator, an external valve block (Figure 4 upper) is employed. To ensure comparability with the specifications of the stock components of the *Active Body Control* system, the bandwidth of the control valve is limited as described in Section 3.2. The valve block has integrated pressure accumulators for the supply and the return lines as well as a pressure sensor in the supply line of the cylinder.

The hydraulic plan of the test rig is depicted in Figure 5: The supplying oil flow of the hydraulic pump is split into two parts for the hydraulic ram of the test rig and the hydraulic suspension actuator. The supply pressure's nominal value for the valve block is $p_V = 200$ bar, which can be adjusted using a pressure reduction valve (see also [2]). A locking valve can be used to disconnect the actuator from the servo valve. The -3 dB-cutoff frequency of the servo valve at

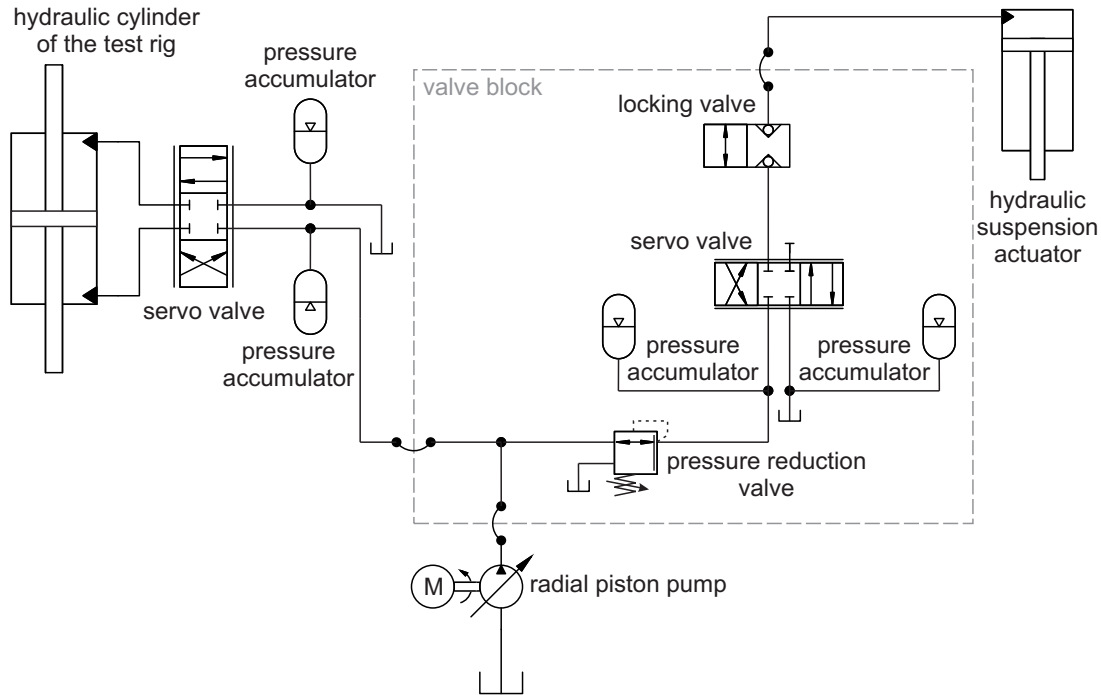


Figure 5: Hydraulic scheme of the test rig.

140 bar valve pressure and $\pm 25\%$ valve opening is approx. 105 Hz.

2.2 Continuously variable damper

The semi-active damper is a continuously variable hydraulic damper with separate valves for compression and rebound direction. By varying the valve currents $\mathbf{i}_d = [i_{d,c} \ i_{d,r}]^T$ for compression and rebound, the damper's force-velocity characteristics can be adjusted as shown qualitatively in Figure 6. If $\mathbf{i}_d = [0 \text{ A} \ 0 \text{ A}]^T$, the hardest characteristic is activated, which represents a fail safe mode.

In the vehicle the damper is controlled via a *FlexRay* bus (see [3]). In the considered application of the hybrid suspension system, the damper control is realized by a power electronic unit instead, that offers BNC connectors for the analog input voltage signals ($\mathbf{u}_{v,cvd}$ proportional to the valve currents) and provides the actual currents in the two valves as output signals.

3 Modeling and control of the actuators

For simulation purposes a detailed nonlinear model of the hydraulic suspension actuator is derived. The corresponding state space model and its experimental validation is presented in this Section. Moreover, the controller design is presented, which utilizes a compensation approach for the static nonlinearities of the hydraulic system and PI-control to assure transparency and robustness of the controller. The dynamic behavior of the controlled hydraulic actuator can be represented by a linear second order model, that is also described in Section 3.2. Although the semi-active damper is a nonlinear dynamic system, its dynamic behavior can be described using static nonlinear characteristics and linear differential equations, which facilitates the feedforward control approach described in Section 3.3. More details on the modeling and control of the hydraulic actuator are presented in [12] and a more detailed damper model is described in [10].

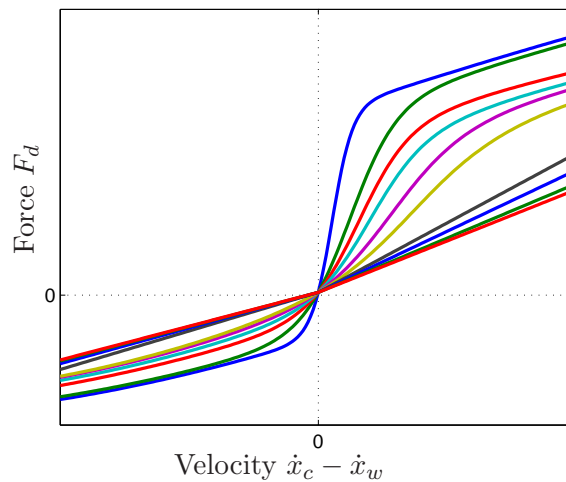


Figure 6: Qualitative characteristics of the continuously variable semi-active damper.

3.1 Hydraulic actuator model

A schematic of the main components of the hydraulic actuator system (valve and piston), that is integrated into the hybrid suspension (see Figure 1), is depicted in Figure 7.

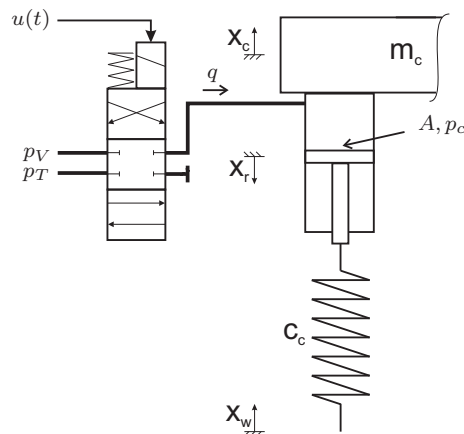


Figure 7: Schematic of the hydraulic low bandwidth actuator system.

For the modeling the hydraulic actuator system is considered in more detail and is therefore structured into 3 parts (see Figure 8):

- The valve: Modeled by an electrical part (relating the input voltage to the position of the valve spool) and a hydraulic part (describing the relation of the pressure at the valve and the corresponding flow rate).
- The tubes: Taking into account the hydraulic capacity and inductance, the pressures and oil flows between the valve and the cylinder are modeled.
- The hydraulic cylinder: The cylinder pressure is related to its movement, which is modeled by a nonlinear third order state space model.

The input signal of the hydraulic actuator is the analog voltage signal $u_{v,hy}(t)$ for the valve, the controlled variable is the actuator position $x_r(t)$, which can be measured. The oil pressure at the actuator rod $p_c(t)$ is also measured to be employed in the controller structure for the hydraulic actuator.

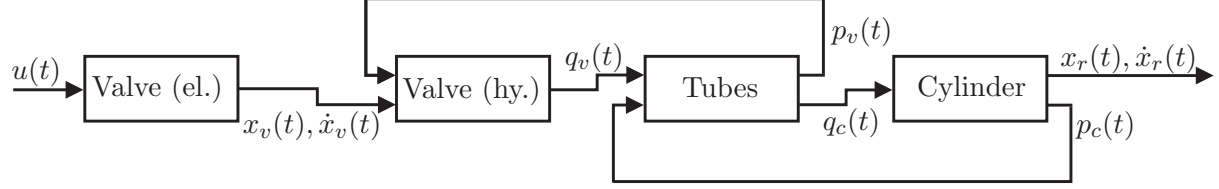


Figure 8: Block diagram of the hydraulic actuator.

Since in the considered application the pressure accumulators are primarily relevant for high frequency dynamics of the hydraulic system (see [12]) and the model order should be kept as low as possible, their influence on the system dynamics is neglected in the model. The resulting nonlinear model has order seven with the states

$$\mathbf{x}_h = [x_{h,1} \ x_{h,2} \ x_{h,3} \ x_{h,4} \ x_{h,5} \ x_{h,6} \ x_{h,7}]^T = [x_r \ \dot{x}_r \ p_c \ p_v \ q_c \ x_v \ \dot{x}_v]^T, \quad (1)$$

where x_r denotes the rod position of the cylinder, p_c , p_v are the pressures at the actuator of the cylinder and the valve respectively, q_c denotes the oil flow into the cylinder and x_v represents the position of the valve piston. Using the parameters defined in Table 1, the input signal $u(t) = u_{v,hy}(t)$ and the measured actuator position $y(t) = x_r(t)$ as output signal the model can be formulated as a nonlinear state space model

$$\begin{bmatrix} \dot{x}_{h,1} \\ \dot{x}_{h,2} \\ \dot{x}_{h,3} \\ \dot{x}_{h,4} \\ \dot{x}_{h,5} \\ \dot{x}_{h,6} \\ \dot{x}_{h,7} \end{bmatrix} = \begin{bmatrix} x_{h,2} \\ \frac{1}{m_r} [A \cdot x_{h,3} - F_c(x_{h,1}) - d_r x_{h,2} - m_r g] \\ \frac{\beta}{V_0 + A x_{h,1}} [x_{h,5} - A \cdot x_{h,2}] \\ \frac{1}{C_h} [\text{sgn}^+(x_{h,6}) k_{sv} \sqrt{|p_V - x_{h,4}|} - \text{sgn}^+(-x_{h,6}) k_{sv} \sqrt{|x_{h,4} - p_T|} - x_{h,5}] \\ \frac{1}{L_h} [x_{h,3} - x_{h,4}] \\ x_{h,7} \\ -\frac{2d_v}{T_v} x_{h,7} - \frac{1}{T_v^2} x_{h,6} \end{bmatrix} + \begin{bmatrix} 0 \\ 0 \\ 0 \\ 0 \\ 0 \\ 0 \\ \frac{K_v}{T_v^2} \end{bmatrix} u$$

$$y(t) = [x_{h,1} \ x_{h,3}]^T$$

$$u(t) = u_{v,hy}$$
(2)

with the linear approximation of the spring force $F_c(x_{h,1}) = c_c x_{h,1} + F_{c,0}$, the hydraulic inductance $L_h = \frac{l_t \rho}{A_t}$, the hydraulic capacity $C_h = \frac{l_t A_t}{\beta}$ and the operator

$$\text{sgn}^+(x_i) = \begin{cases} x_i & \text{for } x_i > 0 \\ 0 & \text{else} \end{cases}. \quad (3)$$

In (2) the relation

$$q_v = \text{sgn}^+(x_{h,6}) k_{sv} \sqrt{|p_V - x_{h,4}|} - \text{sgn}^+(-x_{h,6}) \cdot k_{sv} \cdot \sqrt{|x_{h,4} - p_T|} \quad (4)$$

has been used to eliminate the oil flow through the valve and to express the model by means of the state vector given in (1). The unknown model parameters given in Table 1 have been identified based on measurement data (see [12]) using grey box modeling techniques (see e.g. [7]).

Table 1: Physical quantities and parameters of the hydraulic actuator model

Component	Parameter	Symbol	Value
Oil supply	Supply pressure	p_V	200 bar
	Tank pressure	p_T	2 bar
	Oil elastic modulus	β	$7.12 \cdot 10^8 \text{ N/m}^2$
	Oil density	ρ	888.0348 kg/m^3
Servo valve	Gain (hydraulic)	k_{sv}	$4.1720 \cdot 10^{-8} \text{ m}^{\frac{7}{2}} \text{ kg}^{-\frac{1}{2}}$
	Gain (electromechanical)	K_v	0.4 m/V
	Time constant (electromechanical)	T_v	0.0014 sec
	Damping constant (electromechanical)	d_v	0.8038
	Nominal flow rate	q_{nom}	$40 \cdot 10^{-3} \text{ l/min}$
	Nominal pressure at control edge	p_{nom}	35 bar
	Maximum voltage	$\hat{u}_{v,\text{hy}}$	10 V
Hydraulic cylinder	Piston area	A	$4.7263 \cdot 10^{-4} \text{ m}^2$
	Initial cylinder volume	V_0	$4.3367 \cdot 10^{-8} \text{ m}^3$
	Piston mass (cylinder)	m_r	9.8816 kg
	Friction coefficient	d_r	$7.0006 \cdot 10^3 \text{ Nsec/m}$
	Maximum cylinder stroke	\hat{x}_r	0.0859 m
	Gravitational constant	g	9.81 m/sec^2
Tubes	Tube cross section area	A_t	$3.228 \cdot 10^{-5} \text{ m}^2$
	Tube length	l_t	2.23 m

The model parametrized with the parameter set given in Table 1 is validated using an input signal containing a step sequence with different amplitudes as well as bandlimited white noise (coloured by a first order lowpass filter with 20 Hz cutoff frequency). For the model validation, the model and the real system are controlled by a P-controller (with the gain $k_p = 120$) for the actuator stroke in order to stabilize the system. As can be seen in Figure 9 the model reflects the dynamic behavior of the system well.

3.2 Hydraulic actuator control

The controller structure involves feedforward control of the actuator velocity as well as a PI-feedback controller for the actuator position. In order to be able to compare the influence of different bandwidths of the controlled actuator, a lowpass filter is used for the reference position and the velocity. The controller is tested using the nonlinear model and in experiments. Moreover, it is desirable to find a simple model for the controlled actuator that can be integrated into the simulation model of the hybrid suspension.

3.2.1 Compensation of the pressure dependent valve characteristic The voltage control input u controls the hydraulic actuator by regulating the valve opening. The valve opens and connects the cylinder and the supply pressure tube for $0 < u \leq 10 \text{ V}$ and it connects the cylinder and the tank for $-10 \text{ V} \leq u < 0 \text{ V}$.

For a constant pressure difference, the flow through the valve is proportional to its opening. In the presented application for the controller design the supply pressure is considered to be constant, i.e. $p_V = 200 \text{ bar}$, which is a reasonable assumption due to the high power of the hydraulic pump. Therefore, the pressure difference depends on the actual cylinder pressure p_c , the supply pressure p_V and the opening direction of the 4/3-directional control valve. For

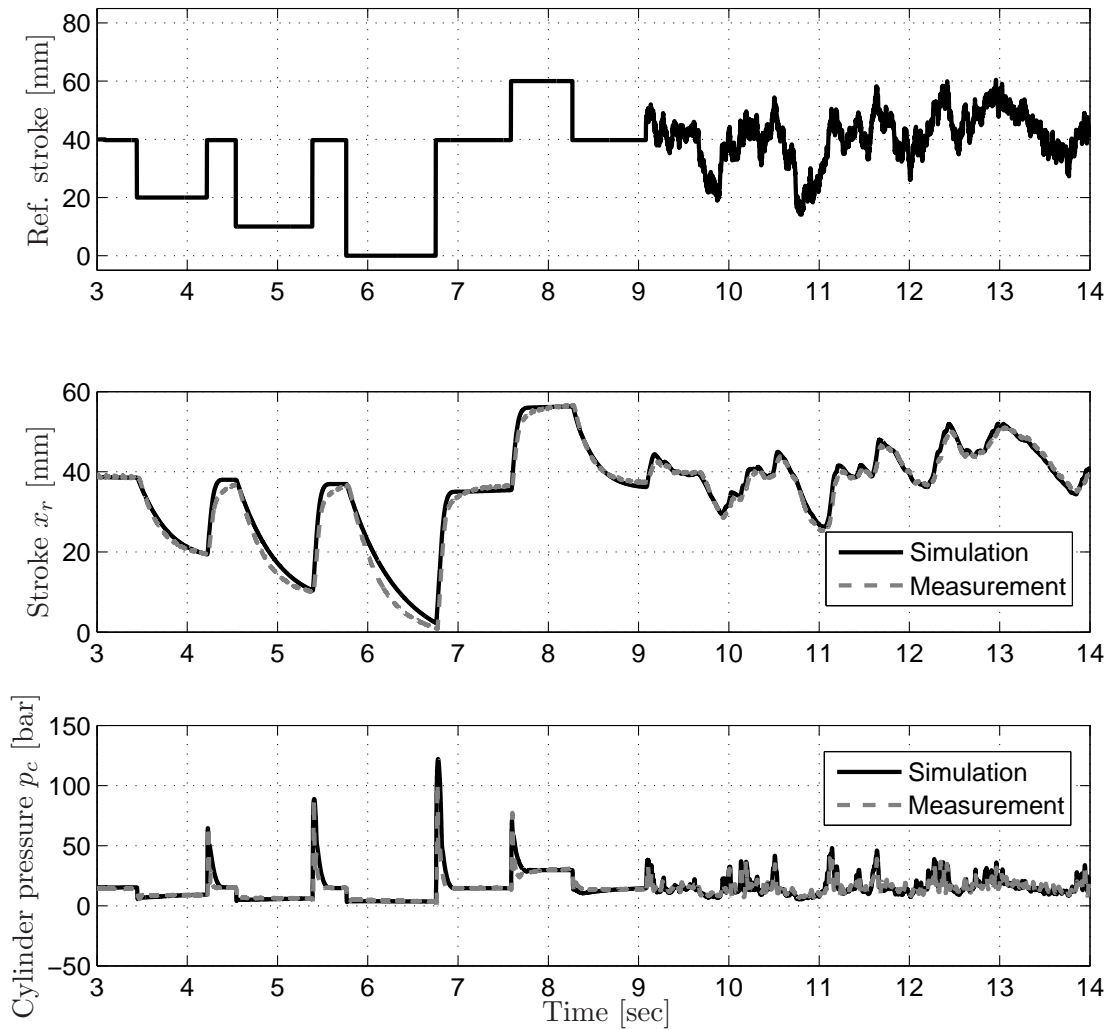


Figure 9: Validation of the hydraulic actuator model (measurement and simulation).

positive oil flow into the cylinder, the relevant pressure difference is determined by the hydraulic supply pressure p_V and the pressure in the cylinder p_c . For negative oil flow from the cylinder to the tank, the pressure drop only depends on p_c as the tank pressure is negligible. The cylinder pressure itself is dynamically coupled to the spring force (in the equilibrium the cylinder pressure equals the spring force divided by the cylinder cross section area) and thus the movements of the actuator and the vehicle suspension. The occurring pressure variations due to the spring deflection and the switching of the valve cause a nonlinear behavior of the valve dynamics: The relation between the valve opening and flow rate is disturbed by the cylinder pressure fluctuations. To compensate this disturbance that influences the valve characteristic, the cylinder pressure p_c is measured and its effects are eliminated by a nonlinear compensation approach scaling the desired control output u^* by a factor depending on the actual value of p_c .

In the equilibrium of the suspension, the valve is closed and the spring induces the pressure $p_{c,0} = 67$ bar in the hydraulic actuator. Thereby, in the equilibrium a reference pressure

$$p_0 = p_V - p_{c,0} = 200 \text{ bar} - 67 \text{ bar} = 133 \text{ bar} \quad (5)$$

is defined, that characterizes the available pressure for generating a positive actuator displace-

ment (spring compression) from the equilibrium by supplying oil to the actuator by the pump. If the spring deflects, p_c changes, which in turn alters the pressure difference on the valve and thereby affects the valve's flow characteristic. For the following considerations, the pressure deviation Δp from the equilibrium pressure p_0 is considered, which depends on the cylinder pressure p_c and on the sign of the valve input signal.

For positive valve input voltages $u \geq 0$, the pressure difference is

$$\Delta p_{pos}(p_c) = (p_V - p_c) - (p_V - p_{c,0}) = p_{c,0} - p_c. \quad (6)$$

If a negative control voltage $u < 0$ is applied, the valve connects the actuator to the tank. Since the tank pressure is negligible and p_V is no longer applied to the actuator, the pressure difference on the valve equals p_c . In the equilibrium $p_c = p_{c,0}$ holds, thus the pressure difference Δp_{neg} in the equilibrium for negative control voltages becomes

$$\Delta p_{neg}(p_c = p_{c,0}) = p_{c,0} - p_0 \quad (7)$$

$$= 67 \text{ bar} - 133 \text{ bar} = -66 \text{ bar}. \quad (8)$$

These resulting pressure differences can be utilized to express the relation between the flow rate \dot{V} and the valve's input signal u as

$$\dot{V} = \left(\frac{\Delta p}{p_0} + 1 \right) \cdot u \cdot c, \quad (9)$$

where c is a constant factor and the pressure deviation from the equilibrium point results from (6) and (8) as

$$\Delta p(p_c) = \begin{cases} \Delta p_{pos} = p_{c,0} - p_c & \text{if } u \geq 0, \\ \Delta p_{neg} = p_c - p_0 & \text{if } u < 0 \end{cases}. \quad (10)$$

This means for negative valve opening in the equilibrium, the valve flow rate would be diminished to approx. half the positive flow rate, i.e.

$$\dot{V} = \left(\frac{\Delta p_{neg}}{p_0} + 1 \right) \cdot u \cdot c = 0.504 \cdot u \cdot c. \quad (11)$$

To get the desired linear relation

$$\dot{V} \stackrel{!}{=} u^* \cdot c \quad (12)$$

between the desired controller output u^* and the flow rate, the measured cylinder pressure p_c is used to calculate the scaled controller output as summarized in Figure 10, i.e.

$$u = \frac{u^*}{\left(\frac{\Delta p}{p_0} + 1 \right)} \quad \text{with } \Delta p = \begin{cases} p_{c,0} - p_c & \text{if } u \geq 0, \\ p_c - p_0 & \text{if } u < 0 \end{cases}. \quad (13)$$

3.2.2 Controller structure The controller structure depicted in Figure 11 realizes the tracking of the actuator displacement $y = x_r$ (the reference displacement is denoted as $w = x_r^*$). Neglecting oil compressibility the actuator velocity depends directly proportional (due to the constant piston area) on the valve flow rate, a feedforward control strategy is implemented utilizing the desired actuator profile velocity. To tune the feedforward gain, a ramp excitation around the equilibrium point has been used to determine the required gains as inverse values of the static plant gains. Thereby, an average gain of $8.9 \frac{\text{V}}{\text{m/sec}}$ for positive velocities and $18.2 \frac{\text{V}}{\text{m/sec}}$

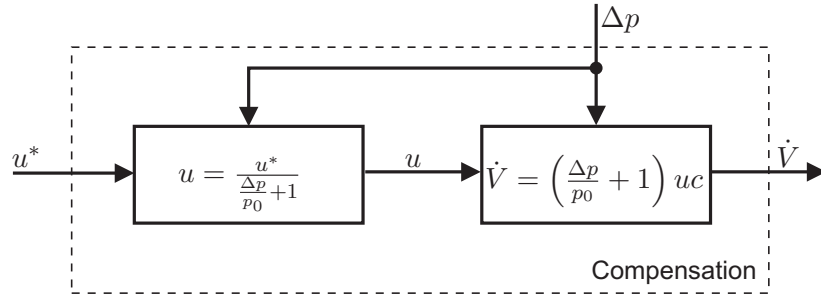


Figure 10: Compensation scheme for the valve nonlinearity

for negative velocities has been identified. The proportion of negative and positive gain coincides with the employed compensation of the valve pressure variations. Thus, for the feedforward control the value $k_f = 8.9$ is used as it refers to the reference pressure p_0 .

The resulting controller structure consists of the velocity feedforward control and a PI-controller (gains $k_p = 650$, $k_i = 1000$) to compensate remaining errors. The feedforward gain is scaled depending on the sign of the control deviation and the actual cylinder pressure as formulated in (13). To avoid a direct coupling of p_c on the feedback gains, the gain of the proportional feedback is scaled only by the static values of Δp at the equilibrium ($p_c = p_{c,0}$) depending on the sign of the control voltage (see (6) and (8)). Since this control leads to a high bandwidth beyond the desired values, lowpass filtering of the reference displacement and velocity is used to be able to adjust the actuator bandwidth in order to study its effects on the suspension performance (w_f denotes the filtered reference displacement). The default bandwidth is chosen to be 5 Hz, which is the original bandwidth of the *Active Body Control System*.

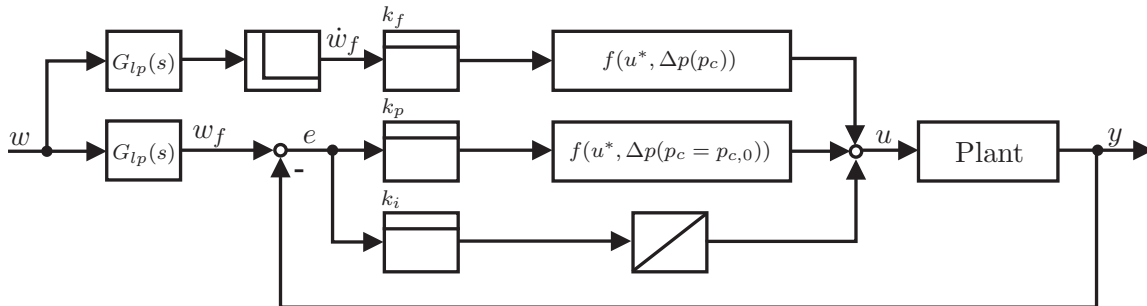


Figure 11: Compensation scheme for the valve nonlinearity

3.2.3 Model of the closed loop system In order to reflect the behavior of the controlled actuator, a simplified model can be utilized. Due to the direct influence of the lowpass filters' cutoff frequency ω_c on the bandwidth of the closed loop system, the dynamics of the controlled actuator can be described in the low frequency range of interest by a second order linear model. Lag effects of the system can be summarized by means of a time delay of $T_d = 3$ msec, which is implemented by a first order Padé-approximation in the model. The resulting model is

$$\dot{\mathbf{x}}_{hy}(t) = \begin{bmatrix} -\omega_c & 0 \\ \frac{1}{T_d} & -\frac{1}{T_d} \end{bmatrix} \mathbf{x}_{hy}(t) + \begin{bmatrix} \omega_c \\ 0 \end{bmatrix} x_r^*(t), \quad (14)$$

$$x_r(t) = \begin{bmatrix} 0 & 1 \end{bmatrix} \mathbf{x}_{hy}(t) \quad (15)$$

with the desired actuator stroke $x_r^*(t)$, $\mathbf{x}_{hy}(t)$ being the state vector of the controlled actuator and the actuator stroke $x_r(t)$ as model output. The model has been proposed by the authors in

[6] and reflects the dynamics of the closed loop system well as can be seen in a comparison of the model output with measurement data (with a bandwidth of 5 Hz) depicted in Figure 12.

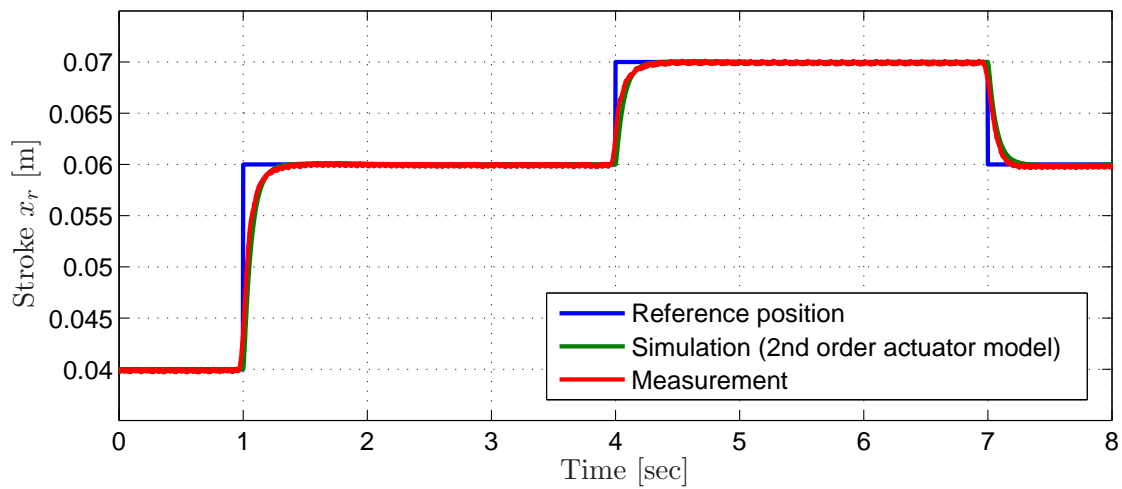


Figure 12: Comparison between measurement and linear second order model for an actuator bandwidth of 5 Hz

3.3 Damper model and control

A model structure (see Figure 15) of the semi-active damper that is suitable for controller design has been published by the authors in [6] and in [4]. Therefore, the approach is only reviewed briefly in this report. The semi-active damper is primarily modeled by its nonlinear characteristic that relates the damper relative velocity $x_c - x_w$ and the valve currents \mathbf{i}_d to the damper force F_d (Figures 6 and 13).

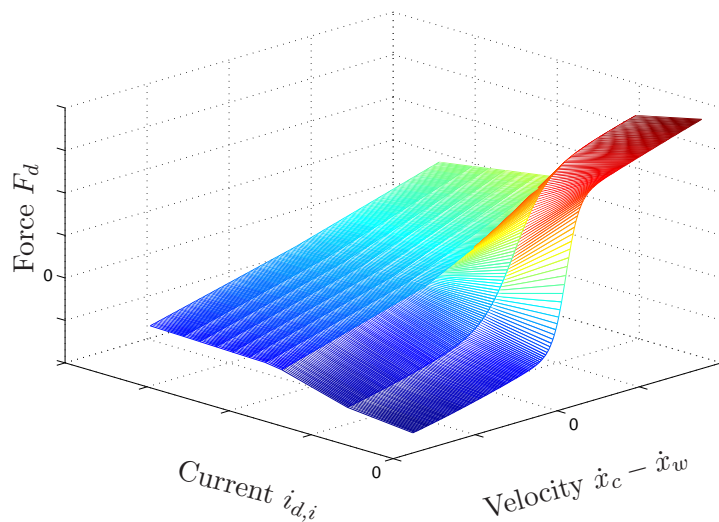


Figure 13: 3D-plot of the semi-active damper characteristics from Figure 6.

Moreover, the dynamic behavior of the damper is described by the transfer functions

$$G_m(s) = \frac{1}{T_{\text{mech}}s + 1}, \quad (16)$$

$$\mathbf{G}_{el}(s) = \begin{bmatrix} G_{el,1}(s) & 0 \\ 0 & G_{el,2}(s) \end{bmatrix} \quad \text{with} \quad G_{el,1}(s) = G_{el,2}(s) = \frac{1}{T_{el}s + 1} \quad (17)$$

with T_{mech} and T_{el} being identified mechanical and electrical time constants of the damper, respectively.

The mechanical dynamics are described by $G_m(s)$ (input signal: static damper force $F_{d,s}$; output signal: actual damper force F_d). The electrical dynamics are characterized by the transfer matrix $\mathbf{G}_{el}(s)$ (input signals: voltage inputs of the power electronic unit $\mathbf{u}_{v,cvd}$; output signals: valve currents \mathbf{i}_d). The damper current signals \mathbf{i}_d are available as measurement signals at the power electronic unit. A more detailed nonlinear physical model of the semi-active damper is presented in [10]. The dependency of the damper's mechanical dynamics on the velocity direction and the current will be analyzed in future work in more detail. The power electronic unit is controlled by an internal PI-controller. The validation of the electrical part of the model is depicted in Figure 14, that shows a step response of the valve currents (model output vs. measured data).

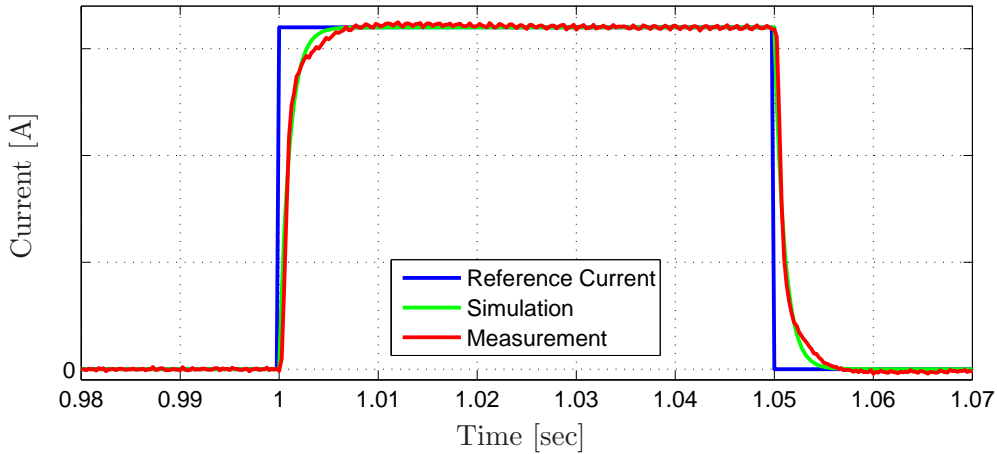


Figure 14: Damper current step response (measurement and simulation).

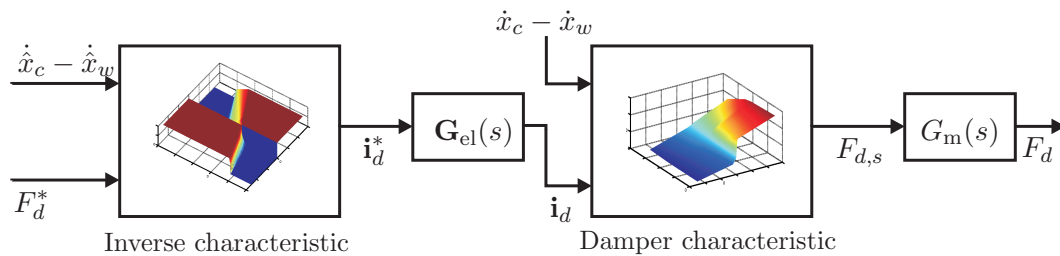


Figure 15: Feedforward control and damper model (see also [6]).

For the control of the damper, a feedforward prefiltering approach using an inversion of the static damper characteristic is employed (see Figure 15). The desired damper force is denoted as F_d^* , the current damper velocity is estimated and denoted as $\hat{x}_c - \hat{x}_w$ (see [4]). The resulting desired damper currents \mathbf{i}_d^* are calculated from the inverse of the three-dimensional damper characteristic in Figure 13 and $F_{d,s}$ represents the static damper force as described by the nonlinear damper

characteristics. Since the damper force is not measured directly, a force control loop can be added based on a damper force estimation, which will be subject of future work.

4 Automotive quarter-car test rig

The hybrid suspension is integrated into a quarter-car test rig (Figure 16), that has been designed to evaluate the performance of suspension control algorithms in a realistic framework. For more detailed information on the test rig, the suspension components as well as modeling and control aspects the reader is referred to [4].

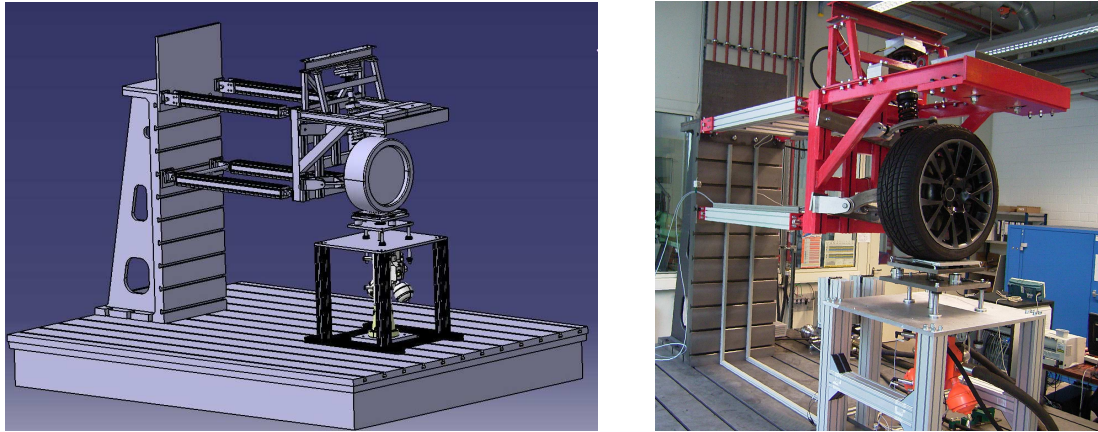


Figure 16: CAD-concept (left) und realization (right) of the hybrid suspension test rig.

The test rig is designed using parameters of the *BMW 7 series* (model year 2009), i.e. the sprung mass is $m_c \approx 500$ kg and the unsprung mass is $m_w \approx 70$ kg. Due to the added length of the hybrid suspension strut, an extension of the test rig frame is used for the mounting of the strut. However, the position and orientation of the hybrid suspension strut is the same as in the *BMW 7 series'* original suspension system, i.e. the kinematic relations of the original suspension configuration including the deflection depending transmission factor (see [8]) are preserved. It is noted that the length of the hybrid suspension strut could be significantly reduced if the damper design is adjusted for its integration into the hybrid suspension setup.

A highly dynamic hydraulic actuator supplied with a pressure of 250 bar is used to excite the tire vertically and thereby emulates the road excitation (see Figure 5). The sprung mass is guided vertically by a parallel kinematics mounting to reduce friction forces. The structure is mounted on a steel base plate resting on 16 airsprings to isolate the building from vibrations.

5 Conclusion and outlook

A realization of a *hybrid suspension* system has been presented. The system involves a continuously variable semi-active damper and a low bandwidth actuator, which is implemented in series to the primary spring of the suspension. The hybrid suspension can be realized using stock hardware of production vehicles. The presented models of the actuators reflect their dynamic behavior well and the transparent control concepts are well applicable in terms of computational complexity for real time application at the test rig. Future work of the authors will involve more complex control schemes for the semi-active damper as well as further study of high-level vehicle suspension control concepts for the hybrid suspension system.

Acknowledgements

The authors would like to thank Thomas Huber for his great input and the realization of the suspension as well as the test rig configuration. Furthermore, the authors would like to thank Carsten Bischoff, Dr. Marcus Jautze, Dr. Markus Nyenhuis and Karsten Röske at BMW AG for providing suspension components and helpful hints to realize the hybrid suspension test rig. The funding support provided by the DFG (German Research Foundation) for the realization of the hybrid suspension test rig and for the project of Nils Pletschen at the Institute of Automatic Control is greatly appreciated. Last but not least, the authors are grateful to all colleagues and students, who have significantly supported the project, especially Christian Rathgeber and Bastian Weigl.

References

- [1] D. Fischer and R. Isermann. Mechatronic semi-active and active vehicle suspensions. *Control Engineering Practice*, 12:1353 – 1367, 2004.
- [2] Herbert Haenchen GmbH. *Datasheet of hydraulic valve block*, 2010.
- [3] M. Jautze, A. Bogner, J. Eggendinger, G. Rekewitz, and A. Stumm. Das Verstelldämpfersystem Dynamische Dämpfer Control. *ATZ extra*, Sonderheft: Der neue BMW 7er:100–103, 2008.
- [4] G. Koch. *Adaptive Control of Mechatronic Vehicle Suspension Systems*. PhD thesis, Technische Universität München, 2011.
- [5] G. Koch, O. Fritsch, and B. Lohmann. Potential of low bandwidth active suspension control with continuously variable damper. *Control Engineering Practice*, 18:1251 – 1262, 2010.
- [6] G. Koch, S. Spirk, and B. Lohmann. Reference model based adaptive control of a hybrid suspension system. *Proceedings of the IFAC Symposium Advances in Automotive Control*, 2010.
- [7] L. Ljung. *System Identification - Theory for the user*. Prentice Hall, USA, 1999.
- [8] W. Matschinsky. *Radführungen der Straßenfahrzeuge - Kinematik, Elasto-Kinematik und Konstruktion*. Springer, 2007.
- [9] M. Mitschke and H. Wallentowitz. *Dynamik der Kraftfahrzeuge*. Springer, Berlin, 2004.
- [10] E. Pellegrini, G. Koch, and B. Lohmann. Physical modeling of a nonlinear semi-active vehicle damper. In *Proceedings of the IFAC Symposium Advances in Automotive Control*, 2010.
- [11] M. Pyper, W. Schiffer, and W. Schneider. *ABC - Active Body Control*. Verlag Moderne Industrie, Augsburg, 2003.
- [12] C. Rathgeber. Modeling and control of an hydraulic actuator for an active suspension. Master’s thesis, Institute of Automatic Control, Technische Universität München, 2010. Supervisor: G. Koch.
- [13] S. M. Savaresi, C. Poussot-Vassal, C. Spelta, O. Sename, and L. Dugard. *Semi-active suspension control design for vehicles*. Butterworth-Heinemann, 2010.